Supplementary Information

(1) **FRAP data** – Table S1 lists the FRAP measurements. FRAP experiments were performed as described previously[1,2]. The measurements have been tabulated as: the number of cells with no detectable signal recovery over the time of observation, number of cells with measurable turn-over, and the fraction of signal recovered in case fluorescence recovery was observed (in parentheses).

(2) **Use of Cse4p-GFP as the reference** – Cse4p-GFP is a stable, core component of the kinetochore, and gets incorporated into the centromeric nucleosome during DNA synthesis[1]. It was therefore used as a reference for deducing the number of metaphase and anaphase/telophase molecules for the rest of the kinetochore complexes from the ratio of the average signal intensity for Cse4p-GFP and a GFP-tagged protein of interest. Cse4p-GFP turn-over within a cluster has been shown to be extremely low in metaphase spindles, both from protein dissociation and kinetochore movement from one spindle half to the other[1]. We verified the stability of Cse4p from metaphase to anaphase/telophase, by comparing the Cse4p-GFP signal in the respective cell phases. The measured ratio for Cse4p-GFP signal (metaphase/anaphase) was 1.07±0.01 (based on 3 experiments). The slightly higher signal in metaphase is the result of the geometrical differences between metaphase and anaphase/telophase spindles. While the centre of the metaphase kinetochore clusters is rarely separated by more than 3 Z planes (with 200 nm increments between steps), the centres of the kinetochore clusters in the longer anaphase/telophase spindles can be separated by as many as 10 Z planes because of the long length of the spindle. By limiting the mean signal to the

measurements from the first 10 Z planes of each stack, we found the metaphase to anaphase/telophase ratio to be 1.0±0.07. The difference in the average signal value for the entire metaphase and anaphase/telophase data sets is also statistically insignificant (t-tests assuming unequal variance yield two-sided p-values of 0.12, 0.15, and 0.27).

(3) **Metaphase intensity distribution in Z for Ask1p-GFP** – Characterization of the intensity distribution for a kinetochore cluster along the Z axis allows us to calculate the step-size dependent error in imaging the maxima in the intensity distribution. With a 200 nm distance (step-size) between successive images, the maximum error will occur when the two images are acquired at 100 nm on either side of the intensity maxima. With the observed intensity distribution shown in Fig. S1, this maximum error will result in an approximately 8% underestimation of the actual value. The average error will result in a 4% underestimation of the measured signal. Fig. S1 shows the average intensity distribution in Z (3 cells) for Nuf2p-GFP in anaphase/telophase (open circles). Measurements for Ask1p-GFP in metaphase are also shown (average of 2 cells, filled circles). To avoid contamination of the intensity distribution of a metaphase kinetochore cluster due to the fluorescence of the sister kinetochore cluster in the other spindle half, one of the kinetochore clusters in the cell was first bleached before carrying out the measurements on the other cluster. As seen from Fig. 2c in the main text and Fig. S1, the intensity distribution for a kinetochore cluster in both metaphase and anaphase/telophase can be approximated by that for a 200 nm fluorescent bead (Fig. 2c in the main text). This is consistent with the geometry of the budding yeast spindle.

(4) **Error arising from the alignment of a pixel array with an imaged kinetochore cluster -** Integration of the imaged intensity distribution with the pixel array of a CCD camera introduces a measurement error that depends on the alignment of the centre of the spot with a pixel in the pixel array. For telophase cells, a 5x5 pixel array was used to cover the spot (143x4 nm). For anaphase/telophase measurements, the maximum intensity pixel was assigned to be the central pixel (3, 3) in the 5x5 pixel box. The maxima of the imaged intensity distribution will rarely align with the centre of one of the pixels introducing an error. The magnitude of this error can be estimated by considering a one dimensional Gaussian intensity distribution. The error will be minimized when the maximum of the Gaussian distribution falls exactly at the centre of a pixel of the CCD array, whereas the maximum error will occur when the maximum of the intensity distribution falls at the edge of two pixels (illustrated in Fig. S2). In reality, the alignment of the maximum of the PSF with a pixel will be uniformly distributed between these two extremes. The average error in the integrated signal will be ~ 2% of the actual signal. The metaphase spot measurements were done using a 6x6 pixel array. The signal measurement box was drawn by assigning the maximum pixel of the image to pixel (4, 4). This introduces a constant error in measurement on top of a variable error similar to the case above. The error amounts to a 9% underestimation of the total signal in the worst case (when the maxima of the Gaussian curve aligns with the edge of the (4, 4) pixel), and a best case error of only 5% (when the maxima aligns with the centre of a pixel). The average error in this case will result in a 7% underestimation.

It should be noted that this estimation was done for a 1-D Gaussian curve in the absence of any noise (background and shot noise). The magnitude of error is proportional to the magnitude of the signal, and its effect will be minimized in a ratio of two averaged intensity values.

(5) **True signal variance** – The distance of the kinetochore cluster away from the coverslip strongly affects the signal magnitude due to spherical aberrations that increase with depth (Fig. 3b in the main text). This effect does not depend on the absolute magnitude of the signal, and thus does not distort the ratio of two fluorescence signals. However, the resultant variation of the signal about the mean signal masks information about the variation in the protein number.

Table S2 lists the mean and standard deviation for three different strains spanning the range of signals measured in this study. We compared the difference in the signal values for the two kinetochore clusters from the same cell that were separated by a Z distance of 400 nm or less. As can be seen from Table S2, the difference in measured intensity values for these kinetochore clusters is small as compared to the total signal. The standard error of the mean fluorescence value based on this difference is also very small. It can be stated in terms of the number of GFP molecules, by using the average Cse4p-GFP signal (1945 counts for 32 GFP molecules at 16 kinetochores -> 60 counts per GFP molecule). Thus, the difference between two kinetochore clusters in the same cell for Cse4p is ~ 4 GFP molecules out of 32, while that for Ndc80p-GFP+Nuf2p-GFP is 20 GFP molecules out of 256. It should also be noted that the standard deviation roughly scales with the mean. This translates into a variation of less than one molecule per kinetochore for each protein.

Because of the suitable spindle geometry of late anaphase/telophase cells, it is possible to accurately measure both signal and background. The geometry of the metaphase spindles forces manual selection of the background region, introducing an additional source of variance in the signal, which is difficult to quantify. The turn-over of all the complexes at the kinetochore is low in metaphase and in telophase. Therefore, the protein number variance in metaphase cells will also be similarly low.

(6) **High background in cells expressing Cep3p-GFP** –The high, inhomogeneous background in cells expressing Cep3p-GFP (Fig. S3) increased the measurement errors in metaphase for this protein. Both Cep3p and Ndc10p also bind spindle MTs in anaphase (Localization for Ndc10p is shown in Fig. 1a). Our measurements for the copy number in anaphase show a decrease in the number of both Cep3p and Ndc10p by the same fraction (a decrease in the ratio from 1.9±0.2 to 1.3±0.01 for Ndc10p and from 0.9±0.2 to 0.6±0.01 for Cep3p – a 1.5-fold decrease in the protein number from metaphase to anaphase in either case).

(7) **Contribution of Ask1p localized to the spindle** – The DAM/DASH complex localizes to kinetochores as well as spindle/interpolar MTs in anaphase. Since it is a MT-associated protein, it may localize to MTs outside of the kinetochore in metaphase. Such DAM/DASH complex molecules not localized to the kinetochore will inflate the measured signal. It is difficult to estimate the amount of DAM/DASH bound to the MTs outside of the kinetochore in metaphase cells due to the near sub-diffraction size of the metaphase half-spindle. We used the fluorescence signal from Ask1p-GFP bound to the anaphase spindles to gauge the magnitude of the signal

contributed by Ask1p-GFP bound to MTs outside of the kinetochore. To estimate the contribution of Ask1p-GFP bound along a MT, we averaged the intensity value over the in-focus sections of the spindle from several cells with an 8 pixel wide line. Each pixel in the kinetochore cluster spot was then assumed to have this average value as the contribution of DAM/DASH bound to non-kinetochore regions of the MTs. Therefore, the average pixel value multiplied by 36 (the area of a 6x6 pixel box used for metaphase signal measurements) was subtracted from the average signal value for the DAM/DASH complex. This calculation reduces the measured number of DAM/DASH complex molecules by 3 or 4. This exercise demonstrates that even after the application of this correction, there is a sufficient number (16 copies) of DAM/DASH complex molecules at the kinetochore to form one ring.

The distribution of Ask1p-GFP fluorescence with respect to the fluorescence for the spindle pole bodies (Spc29-RFP) resembles the distribution of other kinetochore proteins (Fig. S4). This further suggests that most of the Ask1p-GFP remains concentrated at the kinetochores, and not on the spindle MTs.

(8) **GFP response to excitation intensity** – Fig. S5 shows the GFP emission response to excitation intensities. This behavior has been verified for single GFP molecules *in vitro*[3]. The data has been fitted to an equation of the form[3]:

Signal = constant/ (1 + Saturation Intensity/Intensity)

Our protein number measurements were carried out using the highest intensity in Fig. S5 (indicated by the dotted line), which falls in the non-linear response range for the GFP molecules. The non-linear behavior does not affect ratio measurements, as the total signal is the sum of the signal response from each of the individual GFP

molecules in the cluster to the illumination intensity. The non-linear behavior provides some protection against small fluctuations in the epi-illumination due to fluctuations in the arc lamp intensity. Fluorophore bleaching at this illumination intensity and exposure time is minimal (~ 1%). Fig. S5 also displays the linear behavior of the filters and the rest of the microscope optical system. The data was obtained by imaging 200 nm green fluorescent beads at a much lower excitation intensity (~ 0.03x) and integration time (50 ms).

(9) **Variation in the Cse4p-GFP mean signal due to variations in excitation intensity –** The mean signal value for Cse4p-GFP was found to be different for each experiment (Fig. S6). This is most likely due to the changes in the excitation intensity resulting from the differences in the alignment of the arc lamp with respect to the specimen plane (which was done manually), and changes in the arc lamp itself over time. This change in the mean signal value demonstrates the importance of ratio measurements as opposed to relying on the absolute fluorescence signal of a single GFP molecule.

(10) Table S3 provides the raw data for five different proteins from an experiment. Table S4 provides the list of strains used in this study.

(11) **Equipment and Settings –**

Microscope - Nikon Eclipse-TE2000U, 1.4 NA, 100x DIC oil immersion objective.

Filter set – Standard GFP filter set from Chroma.

Camera - Orca ER (Hamamatsu) cooled CCD camera. 12-bit images with 2x2 binning (1 pixel ~ 133 nm) acquired over the central 300x300 pixels of the CCD chip.

Acquisition time - 400 ms for each frame in a 21 frame stack along the Z-direction for each microscope field.

Image acquisition software - MetaMorph 6.1 (Molecular Devices, Downingtown, PA).

Imaging conditions - Cells grown at 25º C in YPD to mid-log phase, re-suspended in SD complete media, and spread on coverslips coated with 0.5 mg/ml of Concanavalin A (Sigma cat. # C7275). Microscopy was done at room temperature.

Image Analysis – Image analysis was carried out with custom written software in MatLAB (Mathworks, Natick, MA) on raw image stacks.

Displayed Images – All the images were acquired with 2x2 binning of the CCD pixel array. The montage in fig. 1a showing metaphase and anaphase spindles was prepared from a representative image for each GFP-tagged protein acquired with 400 ms acquisition time. The intensity range displayed is the same for the metaphase and anaphase panels. The axial intensity distribution for a kinetochore cluster shown in Fig. 2a was reconstructed from 21 planes spaced 200 nm apart using the 3-D reconstruction tool in Metamorph. The average background intensity was also subtracted from the image. Fig. 3c is the maximum intensity projection of five planes spaced 200 nm apart. The gamma value for this image was adjusted so that both, single kinetochores and the kinetochore cluster are clearly visible in the image.

Protein	Metaphase	Anaphase
Ndc10p	12/0	9/0
Ctf19p	8/1(18%)	8/0
Mtw1p	7/1(16%)	6/1(7%)
Nuf2p	9/0	9/1(9.2%)
Ask1p	10/0	6/0

Table S1

	Cse4p-GFP	Nuf2p-GFP	Nuf2p-GFP + Ndc80p-GFP
Complete Data set			
N (clusters)	90	104	104
Average	1945	6796	15523
std. dev.	428	1987	2773
Clusters separated by less than 200 nm			
N (cells)	21	13	23
Average difference	240	840	1195
SEM based on avg. difference	45	232	249

Table S2

TELOPHASE

Protein	N	sigMean	sigDev	bkgMean	bkgDev	z1Mean	z1Std	N1	z2Mean	z2Std	N2
Cse4p-GFP	90	1945	429	6550	430	2215	663	17	2021	289	44
Ndc10p-GFP	64	2550	677	7263	464	3651	489	7	2775	360	24
Ctf19p-GFP	70	2912	681	7314	463	3453	684	27	2748	415	23
Mtw1p-GFP	98	6258	1857	7256	572	7691	2045	14	6618	1480	48
Nuf2p-GFP	78	6797	1988	7609	603	8323	1905	16	6886	1776	35
Ask1p-GFP	64	5911	1212	7968	795	6803	1252	11	6172	1031	24

METAPHASE

Protein	N	sigMean	sigDev	bkgMean	bkgDev	z1Mean	z1Std	N1	z2Mean	z2Std	N2
Cse4p-GFP	28	2419	529	10251	1538	2697	33	2	2148	574	10
Ndc10p-GFP	34	4070	1443	11132	879	5336	1596	7	3742	1262	25
Ctf19p-GFP	70	2912	681	7314	463	3453	684	27	2748	415	23
Mtw1p-GFP	22	6831	1832	9928	208	7531	897	4	6737	1988	16
Nuf2p-GFP	22	9327	1608	10728	1050	10330	1753	6	8951	1430	16
Ask1p-GFP	18	24487	7817	11319	1167	29320	4038	3	24036	8163	14

Table S3 lists the representative data sets for each of the proteins considered in this study. It should be noted that the data sets for Cse4p-GFP and Nuf2p-GFP come from the same experiment, thus making ratio calculation meaningful for the pair.

N = total number of measurements

sigMean = Mean Signal

sigDev = standard deviation for the measured signal

bkgMean = Mean background

bkgDev = standard deviation for the background

z1Mean(z2Mean) = mean signal for measurements done in the 1-5(6-10) Z planes

z1Std(z2Std) = corresponding standard deviation

N1, N2 = Number of measurements for the respective subgroups

Strain	Genotype	Source
KBY7006	YEF 473a Cse4-GFP:KAN^R	Bloom lab
KBY2310	YEF 473a Ndc10-GFP:HIS	Bloom lab
DCB110	YEF 473a Cep3-GFP:HIS	Bloom lab
KBY7013	YEF 473a Mif2-GFP:KAN^R	Bloom lab
KBY7009	YEF 473a Ctf19-GFP:KAN^R	Bloom lab
SWY40B	S288C MATα *his3 200, leu2-3,112, ura3-52, lys2,* Mtw1-GFP:KAN^R	Drubin Lab
KBY5056	YEF 473a Nuf2-GFP:HB^R	Bloom lab
KBY7005	YEF 473a Ndc80-GFP:KAN^R	Bloom lab
ICY211D	S288C MATα his3 200, leu2-3,112, ura3-52, lys2, Ask1-GFP:KAN^R	Drubin Lab
KBY7012	YEF 473a Ctf3-GFP:KAN^R	Bloom lab
KBY4014	9c MATa, *ura3, leu2,* Chl4-GFP:KAN^R	Bloom lab
KBY7016	YEF 473a Nkp2-GFP:KAN^R	Bloom lab
KBY7008	YEF 473a Nuf2-GFP:HB^R Ndc80-GFP: KAN^R	Bloom lab
KBY4139	J178D His4::Gal-CEN:HB^R Nuf2-GFP:URA3	Bloom lab

Table S4

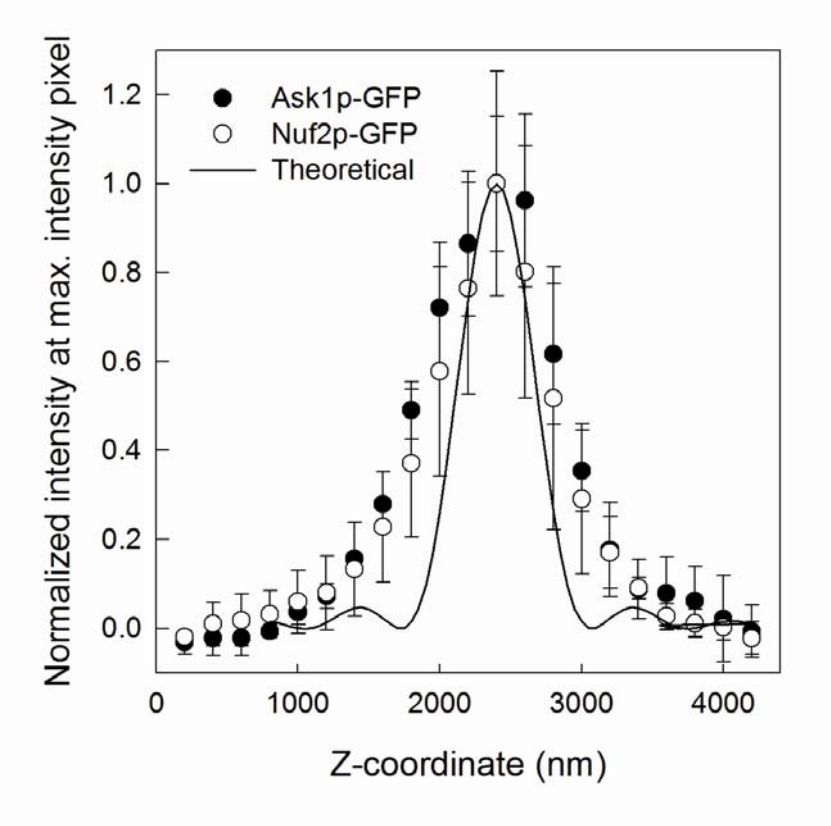

Figure S1

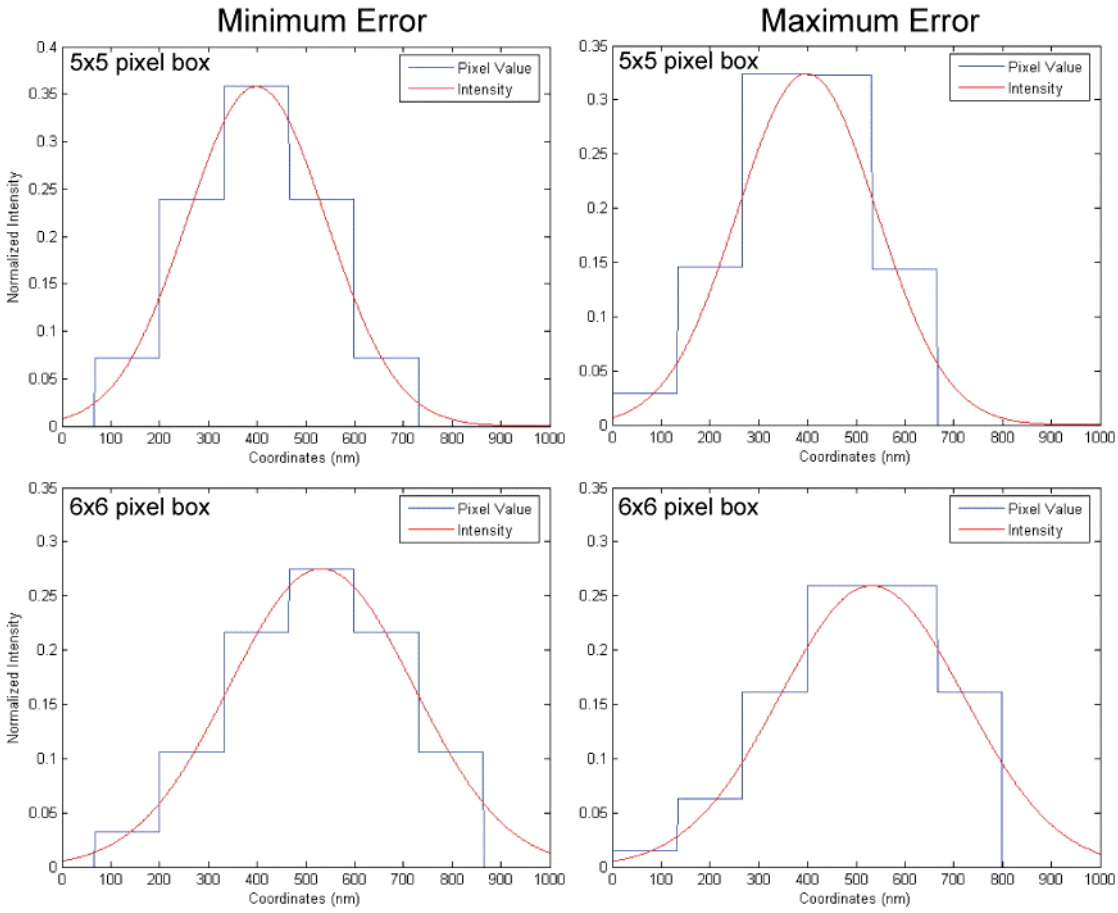

Figure S2

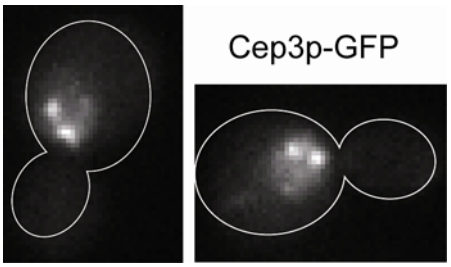

Figure S3

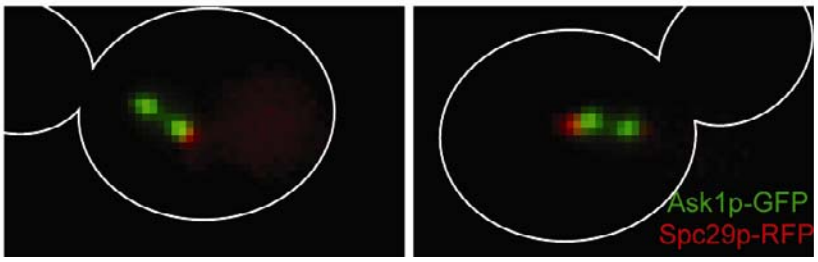

Figure S4

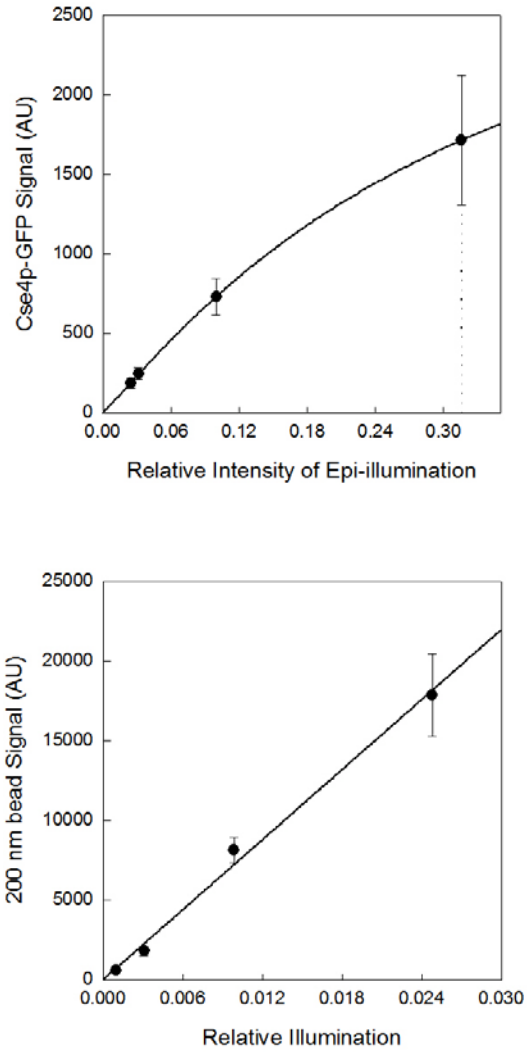

Figure S5

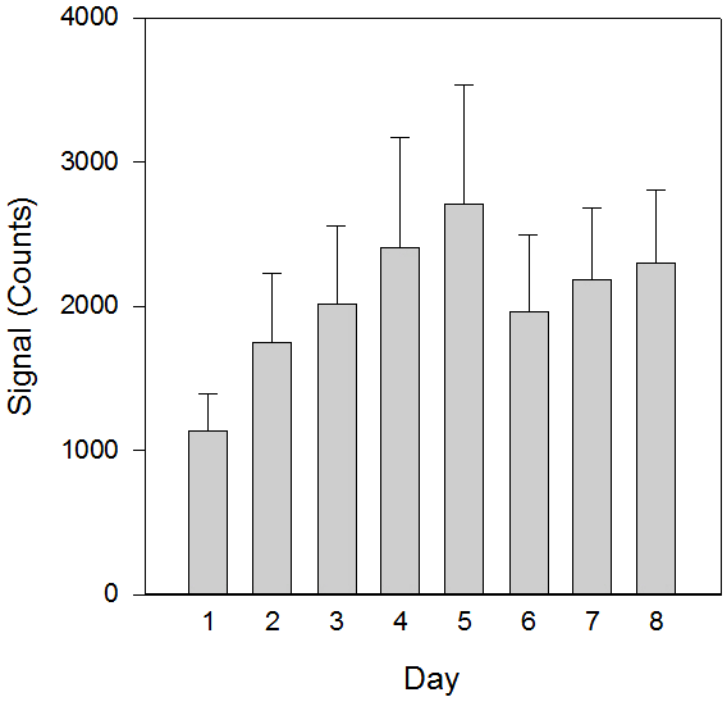

Figure S6

REFERENCES

1. Pearson, C. G. et al. Stable kinetochore-microtubule attachment constrains centromere positioning in metaphase. *Curr Biol* **14**, 1962-7 (2004).
2. Roumanie, O. et al. Rho GTPase regulation of exocytosis in yeast is independent of GTP hydrolysis and polarization of the exocyst complex. *J Cell Biol* **170**, 583-94 (2005).
3. Kubitscheck, U., Kuckmann, O., Kues, T. & Peters, R. Imaging and tracking of single GFP molecules in solution. *Biophys J* **78**, 2170-9 (2000).